

SHELL AND ODD-EVEN EFFECTS IN PREEQUILIBRIUM NUCLEON EMISSIONS
IN THE CONTINUUM FROM NUCLEON-INDUCED REACTIONS

Y. Watanabe, I. Kumabe, N. Koori, and M. Hyakutake*

Department of Nuclear Engineering, Kyushu University, Fukuoka 812, Japan

Abstract: We have investigated the shell and odd-even effects in preequilibrium particle emissions in the continuum from (p,p'), (n,n'), (p,n), and (n,p) reactions. Double differential cross sections were measured for 18-MeV(p,xp) reactions on ^{90}Zr , ^{93}Nb , $^{92,94,96,98,100}\text{Mo}$, ^{106}Pd , and Ag, and for 14.1-MeV(n,xn) reactions on Ag, Cd, In, Sn, Sb, and Te. The shell and odd-even effects were not appreciably observed in the preequilibrium (p,p') and (n,n') spectra in excitation energies above 4 MeV. This was reasonably interpreted on the basis of the state densities generated from the Nilsson model and the modified uniform spacing(MUS) model. Neutron energy spectra from 25-MeV (p,n) reactions on nuclei in the Zr-Mo and Cr-Ni regions were analyzed in terms of the exciton model in which the effective Q value and the state densities generated from the MUS model were employed and the pairing correlation was taken into account. The calculated spectra showed good agreement with not only the experimental ones in the continuum region of 12-18 MeV, but also those with pronounced structures above 18 MeV. The same model was also applied to the analyses of 18-MeV (p,n) reactions and 14-MeV (n,p) reactions.

(nucleon induced reaction, preequilibrium process, shell and odd-even effects, state density, effective Q value)

Introduction

In nuclear reactions induced by neutrons of several tens of MeV, preequilibrium process becomes a significant reaction mechanism. Most of fusion reactor candidate materials are metals or their alloys which consist of atoms with nuclei near the shell closure. Investigation on shell and odd-even effects in the preequilibrium process, therefore, is of great importance for enhancing our understanding of the reaction mechanism as well as for meeting nuclear data needs for fusion energy applications.

For such investigation, it is an effective approach to utilize proton induced reactions that are analogous to neutron induced reactions, because experimental data of the former are superior to those of the latter in terms of counting statistics. Detailed information on the preequilibrium process will be derived through the unified understanding of (N,N) reactions, where N denotes the nucleon.

In the present work, double differential cross sections were measured systematically for 18-MeV (p,xp) reactions on ^{90}Zr , ^{93}Nb , $^{92,94,96,98,100}\text{Mo}$, ^{106}Pd , and Ag in order to study the preequilibrium process in inelastic scatterings¹. Another measurement of 14.1-MeV (n,xn) spectra² have been performed for Ag, Cd, In, Sn, Sb, and Te in order to examine the similarity between (p,p') and (n,n') scatterings with respect to the shell and odd-even effects in the preequilibrium process. In addition, 18-MeV and 25-MeV (p,n) spectra and 14-MeV (n,p) spectra for nuclei in the Zr-Mo and Ti-Cu regions were analyzed on the basis of the exciton model introducing the effective Q value.^{3,4}

18-MeV (p,p') scattering

The experiment¹ was performed using an 18 MeV proton beam from the tandem Van de Graaff accelerator at Kyushu University.

Figure 1 shows the measured angle-integrated (p,xp) spectra for all target nuclei. The proton

spectra for shell closed nuclei (^{90}Zr and ^{92}Mo) with neutron number 50 have noticeable structures in outgoing energies above 10 MeV. On the other hand, the spectra for nuclei away from the shell closure become flat and smooth with increasing neutron number, and have a similar shape and almost the same magnitude within several percent in the preequilibrium region above 10 MeV.

Part(a) and (b) in Fig.2 shows the cross sections(σ_a and σ_b) integrated over 10-13 MeV after subtraction of the equilibrium component estimated in two ways; (a) one is the calculated cross section using the Hauser-Feshbach model, (b) the other is the measured cross section at a backward angle $\theta=160^\circ$. Although the absolute values of the nonequilibrium cross sections σ_a and σ_b are different, each is nearly equal within the error among the measured isotopes. Consequently, there are no appreciable shell and odd-even effects in the (p,p') spectra in the outgoing energy region corresponding to excitations above 4 MeV, where preequilibrium emissions are dominant.

This fact was reasonably interpreted on the basis of the state densities generated from two sets of single particle levels using the recursion method⁵; one is based on the spherical Nilsson model⁶ and the other on the modified uniform spacing (MUS) model³ in which a shell gap is introduced into the uniform spacing (US) model. The pairing correlation was taken into account under the quasi-particle approximation. As shown for $^{92,96,100}\text{Mo}$ in Fig.4, the influence of a shell gap on the calculated (n)(n)⁻¹ state densities for the neutron shell is reduced significantly in excitation energies above 4 MeV. For an odd- and even-A pair of ^{107}Ag and ^{106}Pd , the (p)(p)⁻¹ state densities were also calculated by the same method as mentioned above.¹ The difference between both the state densities appeared below ~ 2 MeV, where the states are mainly created by excitations of an unpaired proton. However both were almost equal above ~ 2 MeV, because excitations associated with pairs of nucleons are dominant.

The emission from n=3 initial configuration in the composite nucleus has a large fraction in

* Present address: Sasebo Technical College, Sasebo 857-11, Japan

the preequilibrium emissions. According to the exciton model, the energy spectrum of emitted particles from $n=3$ is proportional to the $1p-1h$ state density of the residual nucleus. It can be, therefore, understood from the above discussion on the state density that there are no appreciable shell and odd-even effects in the preequilibrium (p,p') spectra.

As shown in Fig.3, the MUS model reproduces well the averaged behavior of the state densities obtained from the spherical Nilsson model in excitations above 4 MeV. This indicates that the Williams formula commonly used in the preequilibrium models is a reasonable approximation above 4 MeV even for nuclei near the shell closure.

Furthermore, the measured angle-integrated proton spectra were compared with those calculated on the basis of the exciton model and the Hauser-Feshbach model in which the isospin selection rule was taken into account¹. Good agreement between the experimental and calculated spectra was obtained in the continuum region of 3-14 MeV for all targets.

14.1-MeV (n,n') scattering

The experiment was performed with a TOF spectrometer using a 14.1 MeV pulsed neutron beam at OKTAVIAN in Osaka University.²⁻⁷

Double differential neutron emission cross sections measured at 70° are shown for Ag, Cd, In, Sn, Sb, and Te in Fig.4. In the energy region of 5-10 MeV, where the preequilibrium emission is dominant, the measured spectra are similar in shape except for Te. The (n,xn) spectrum for Te has such structure that some small peaks overlap, and the magnitude is somewhat larger than those for the other spectra.

In Fig.4, the experimental spectra are compared with $1/4\pi$ of the angle-integrated spectra calculated on the basis of the evaporation model and the exciton model.² The calculated spectra are in good agreement with the experimental ones in the outgoing energy region of 1-10 MeV, although some underestimation is seen in 7-10 MeV for Te.

The experimental cross sections integrated over 7-10 MeV at 70° are shown by the solid circles in Fig.5. The cross sections increase monotonically with increasing mass number from Ag to Sb. However the cross section for Te increases

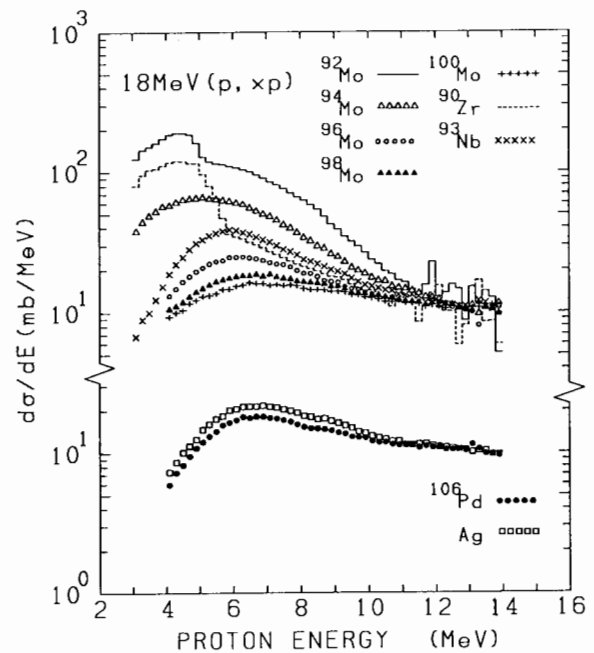


Fig. 1. Angle-integrated energy spectra of protons emitted from 18 MeV (p,xp) reactions

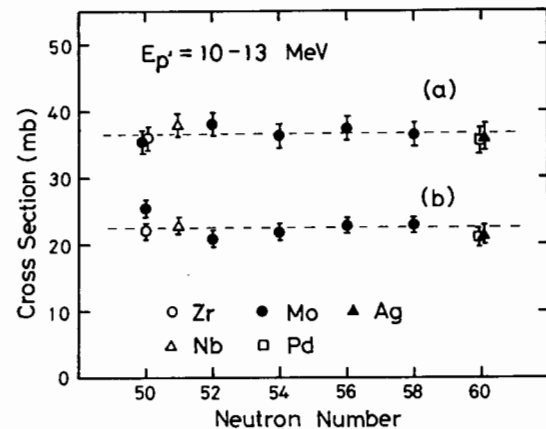


Fig. 2. Nonequilibrium cross sections integrated over 10-13 MeV after subtraction of equilibrium component.

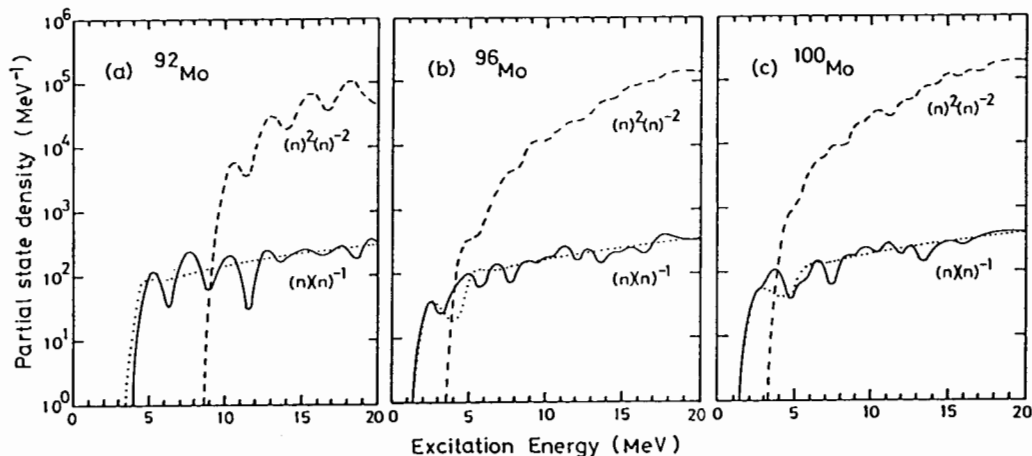


Fig. 3. Partial state densities for $1p-1h$ and $2p-2h$ neutron configurations. Solid and dashed curves represent state densities generated using the spherical Nilsson model. Dotted curves are the results of the modified uniform spacing model.

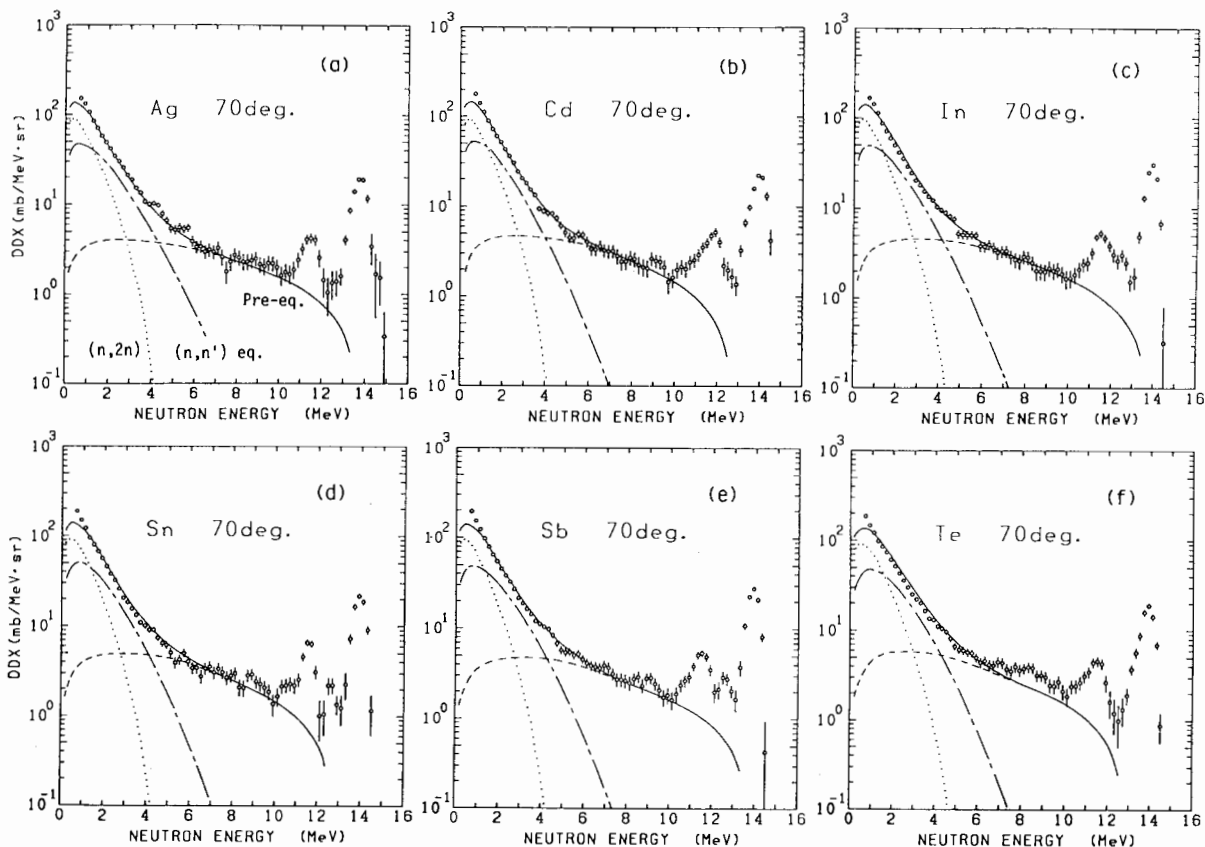


Fig. 4. Comparisons of the experimental and calculated double differential neutron emission cross sections for Ag, Cd, In, Sn, Sb, and Te. Dashed curves are the calculated preequilibrium spectra. Dotted-dashed curves and dotted curves show the calculated evaporation spectra for (n,n') and (n,2n) reactions, respectively. Solid curves are the sum of them.

discontinuously.

To interpret the discontinuous increase for Te, we estimated the contribution of the direct collective excitation of the low energy octupole resonance (LEOR) by using experimental values of the deformation parameter β_3 for the first 3^- state and the systematics for E3 transitions.² The cross sections after subtraction of the LEOR cross section from the experimental ones are shown by open circles in Fig. 6. The resulting cross sections showed no appreciable shell and odd-even effects. This component may be assumed to be the preequilibrium component, because excitations of the coherent motion such as the LEOR can not be treated in the framework of the preequilibrium model such as the exciton model.⁹

The components of direct process may also be included in the continuum region of (p,p') spectra. Similarly, we calculated the σ_{LEOR} for the (p,p') scattering by nuclei in the Mo region, and obtained the preequilibrium components from subtraction of the σ_{LEOR} . The results also led to a consistent conclusion with that of the (n,n') scattering.

(p,n) and (n,p) reactions

The 25-MeV (p,n) spectra for Zr-isotopes measured by Scobel et al.¹⁰ are shown by histograms in Fig. 6. Each spectrum has structureless continuum in the outgoing energy region, where the preequilibrium process is dominant, except for isobaric-analog-state (IAS) peaks.

For nuclei with a given atomic number, the preequilibrium (p,n) cross sections increase with

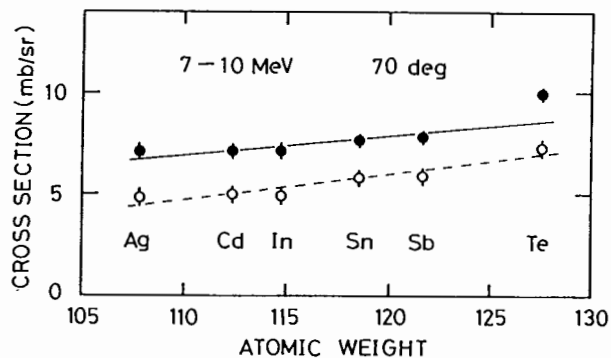


Fig. 5. Dependence of integrated cross sections over 7-10 MeV on the atomic weight of scatterers.

increasing Q value according to the exciton model³. Figure 6 indicates that the cross sections in the 12-18 MeV region increase smoothly with increasing mass number, regardless of a large difference of the true Q values between the shell closed nucleus ^{90}Zr and the odd nucleus ^{91}Zr . Namely, the shell and odd-even effects are not appreciably observed in the continuum portion of (p,n) spectra as well as (p,p') and (n,n') spectra. This trend is expected to be reproduced by the exciton model calculation using the effective Q value³ which is a smooth function of mass number for a given atomic number and is shell-independent.

In Fig. 6, the experimental (p,n) spectra are compared with those calculated in terms of the exciton model with the effective Q value and the true Q value, respectively. In both the

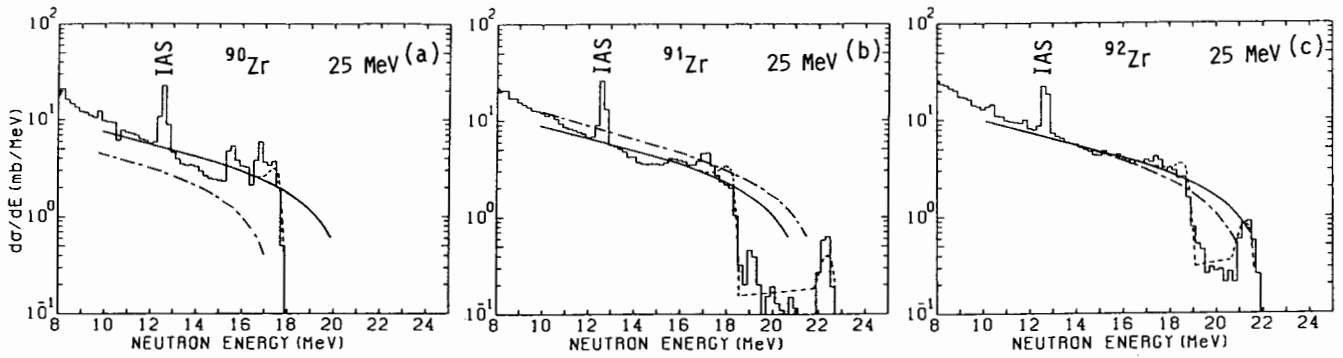


Fig. 6. Calculated and experimental angle-integrated energy spectra for 25-MeV (p,n) reactions on Zr-isotopes.

calculations, the Williams formula based on the US model was used as the state density. The calculated spectra using the effective Q value (solid curves) show better agreement with the experimental ones than those using the true Q value (dotted-dashed curves).

Next, the state densities generated from the MUS model were employed in place of the Williams formula for 1p-1h states of the residual nucleus. The pairing correlation was also taken into account under the quasi-particle approximation. The details of the calculation have been described in Ref.3. Comparisons of the experimental and calculated (p,n) spectra are shown by dashed curves in Fig.6. The calculated spectra are in good agreement with not only the experimental ones in the energy region of $E_n = 12-18$ MeV, but also those with pronounced structures in the region of $E_n > 18$ MeV.

The same model was applied to the analysis of 14-MeV (n,p) reactions on nuclei in the Zr-Mo region.⁴ As shown in Fig.7, the (n,p) spectra calculated using the MUS model and the effective Q value (double dot-dashed curves) show better agreement with the experimental ones¹¹ than those using the US model and the true Q value (dotted curves).

Finally, the energy spectra from the 25-MeV (p,n) reaction on nuclei in the Cr-Ni region¹⁰ and the 14-MeV (n,p) reaction on nuclei in the Ti-Cu region¹² were analyzed in terms of the same exciton model as mentioned above.⁴ The calculated spectra showed fairly good agreement with the experimental ones.

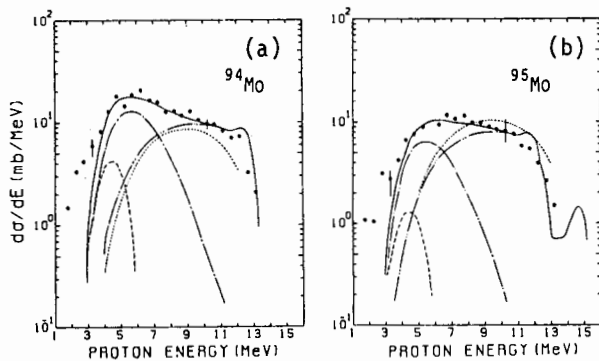


Fig. 7. Calculated and experimental angle-integrated energy spectra for 14-MeV (n,p) reactions on ^{94,95}Mo. Dotted-dashed curves and dashed curves are the calculated evaporation spectra for (n,p) and (n,np) reactions, respectively. See text for double dotted and dashed curves and dotted curves.

Summary

The preequilibrium particle emissions in the continuum from the (N,N) reactions have been studied with special attention to the shell and odd-even effects. It was found that there were no appreciable shell and odd-even effects in the continuum (N,N) spectra, except for the high outgoing energy portion and structure with the peaks or the bumps corresponding to direct collective excitations (e.g. the LEOR and the IAS). These observations were interpreted in terms of the state densities generated from realistic single particle level schemes introducing a shell gap under the quasi-particle approximation. Furthermore, it was confirmed from the analyses of the (p,n) and (n,p) spectra that the effective Q value was available in the preequilibrium calculations based on the exciton model.

The authors would like to thank members of the Nuclear Physics Laboratory of the Department of Physics, Kyushu University, and Dr. A. Takahashi and his co-workers of the OKTAVIAN facility, Osaka University, for their assistance in operating the accelerator.

REFERENCES

1. Y. Watanabe et al.: Phys. Rev. C **36**, 1325 (1987).
2. Y. Watanabe et al.: Phys. Rev. C **37**, 963 (1988).
3. I. Kumabe and Y. Watanabe: Phys. Rev. C **36**, 543 (1987).
4. I. Kumabe et al.: JAERI-M 88-065, p.212 (1988).
5. F.C. Williams, Jr. et al.: Nucl. Phys. **A207**, 619 (1973).
6. S.G. Nilsson: Mat. Fys. Medd. Dan. Vid. Selsk., **29**, No.16 (1955).
7. A. Takahashi et al.: J. Nucl. Sci. Technol. **25**, 215 (1988).
8. F.C. Williams, Jr.: Nucl. Phys. **A166**, 231 (1971).
9. P.E. Hodgson et al.: Proc. Int. Conf. on Nuclear data for Basic and Applied Science, Santa Fe, May 13-17, 1985 (Gordon and Breach Science Pub., 1986), Vol.2, p.1033.
10. Scobel et al.: Phys. Rev. C **30**, 1480 (1984).
11. S.M. Grimes et al.: Nucl. Sci. and Eng. **62**, 187 (1977); Phys. Rev. C **17**, 508 (1978).; *ibid.*, C **19**, 2127 (1979).
12. R.C. Haight et al.: Phys. Rev. C **23**, 700 (1981).